CBN 00-7
CBX 00-28
M.Dubrovin
D.Cinabro
25 April 2000

CLEO Silicon PIN-Diode Radiation Monitor System: CLEO III Engineering Run

1 Introduction

The CLEO radiation monitor system that was used during the CLEO III engineering run, October 1999 through February 2000, is reviewed. We describe the upgraded PIN-Diode Radiation Monitor system. We have paid much attention to the calibration, understanding its stability, and the precision of the dose measurement. Only a slightly altered system is used for the CLEO III physics run.

2 Location of sensors

The detectors of the PIN-Diode Radiation Monitor consists of 24 PIN diodes (Siemens, type SFH 206K) which are located in two aluminum rings at a radius of 2.4 cm from the beam axis shown in Figure 1 and at a distance ±14 cm to the west and east of the

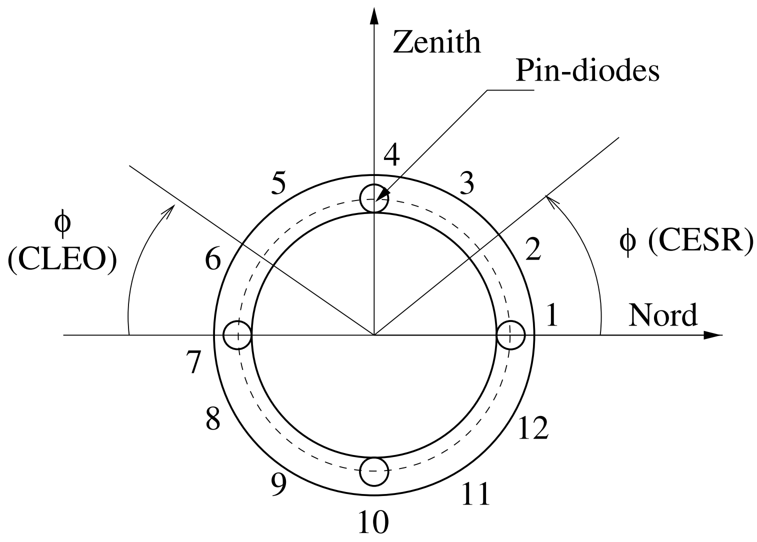

Figure 1: PIN-diode orientation and numbering in their retainer rings.

interaction point. On each side the monitors are numbered from 1 to 12, with 1 being on the north (inside of the CESR ring), 3 being on the top, etc.

3 Electronics

The general scheme of the electronics for each of the 24 channels is shown in Figure 2. To extend the dynamic range of the monitor by a factor of 10 the output is split into two

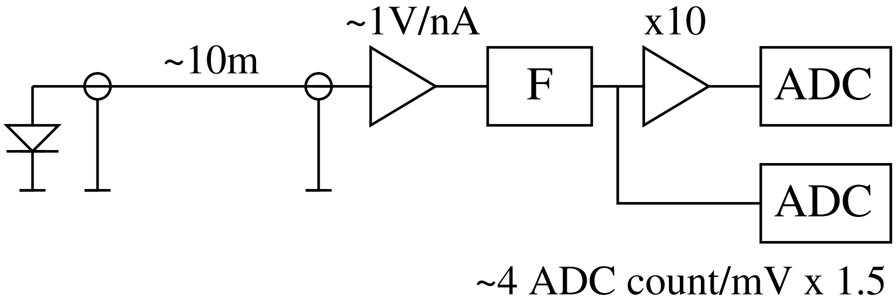

Figure 2: General scheme of the PIN-diode radiation monitor electronics.

parts; one that passes through a second gain stage (x10) and another with no change to the initial gain. A detailed schematic of the integrating amplifiers is shown in Figure 3. The output of the amplifiers goes to a filter whose schematic is shown in Figure 4. Two

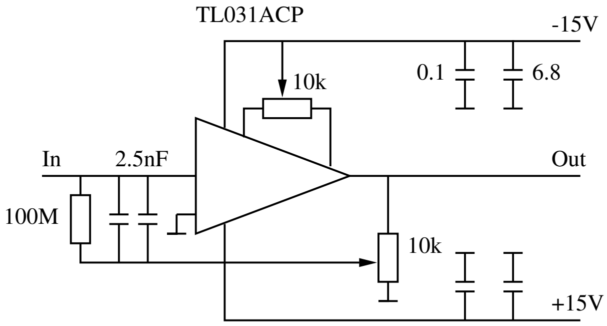

Figure 3: Schematic of the integrating amplifier.

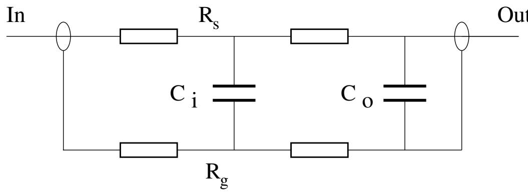

Figure 4: Schematic of the filter.

simple circuits shown in Figure 5 and Figure 6 are used for calibration of channels in

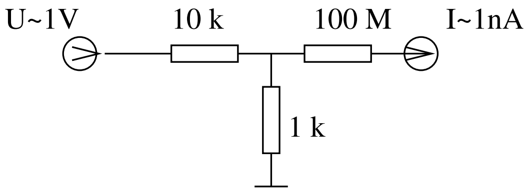

Figure 5: Calibration circuit for current mode.

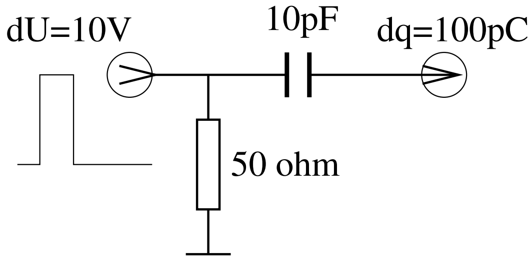

Figure 6: Calibration circuit for charge mode.

current amplification and charge amplification mode respectively.

4 Software

Several stand-alone routines related to Radiation Monitors are located at CESR24 computer in the directory USER$DISK:[CLEO21.CLEOSIRAD].

Three new routines have been developed to have easy access to Radiation Monitor data:

- RDB.* reads the contents of several files stored in the CESR data base. Record are stored in the data base at the rate of one per minute. The program extracts more than 100 parameters, and puts them in Ntuple RADMON.TUP. The program reads the records for a specified day.
- ROL.* creates the same Ntuple RADMON.TUP, but reads the radiation monitors on-line, with a rate of one record per second. The number of records to read is inquired at the start of the routine.
- DOSEINT.* integrates the accumulated dose between two dates specified at start of the routine. Differential and integrated dose for each channel and their average value are stored in Ntuple DOSEINT.TUP, one record per day.

Several helpful PAW scripts (KUMAC-files), located in the daughter directory USER$DISK:[CLEO21.CLEOSIRAD.PAWIAN], allow us to have convenient access to the above Ntuples and draw graphical pictures of monitor response.

5 Calibration

The small value of the measured currents from the PIN diodes and the high gain of the amplifiers imply that careful attention must be given to calibration. The first approach placed an additional resistor of 1 Mohm parallel to the amplifier input to generate a small current signal. This shifted the output base level $> 100\%$ with respect to the signal. To eliminate the influence of the circuit on the calibration the resistor has been increased up to 100 M. Dynamic calibration has been also done to insure that the calibration circuit does not change the gain of the amplifier.

5.1 Measurement of injected test current

Injected current, generated by the circuit shown in Figure 5, is measured with a picoampmeter as a function of input voltage. Figure 7 shows the linearity of the response and the residuals from the linear fit. The residuals demonstrate, that the injected current can be adjusted with a precision of ~ 1 pA. Based on the calculated PIN-diode response current for different "round values" of radiation dose, the corresponding input voltages have been chosen. The results are listed in Table 1.

5.2 Components of the filters

To check that the filters, shown in Figure 4, are in a good working condition, their parameters have been measured separately. The results are listed in Table 2.

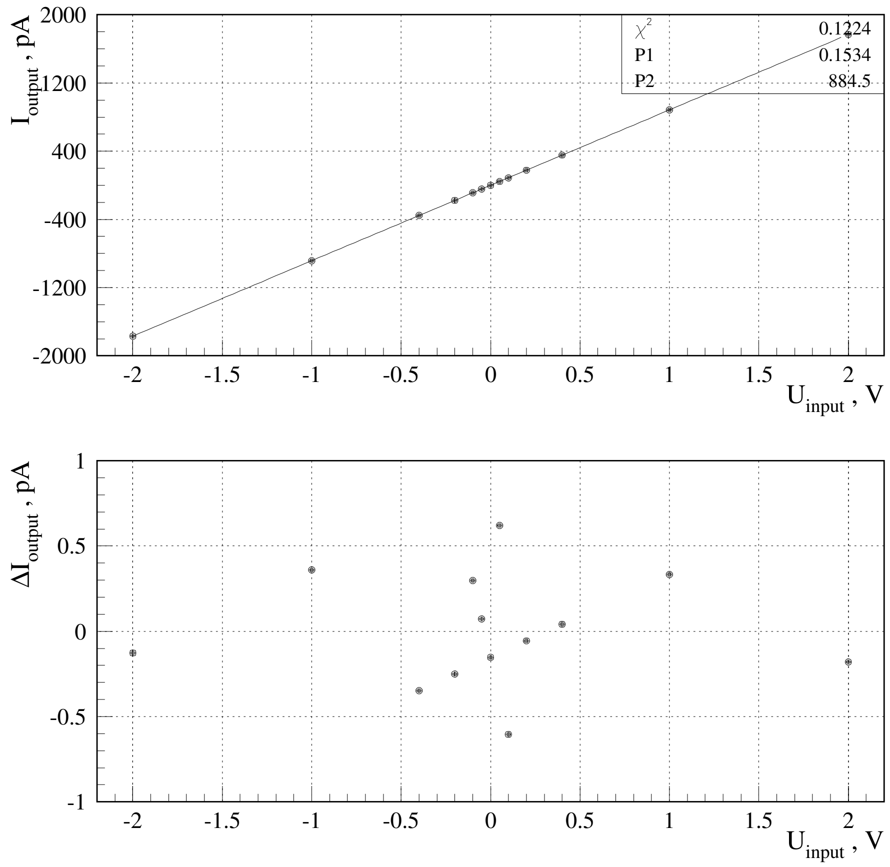

Figure 7: Dependence of the injected current, and residuals from the linear fit shown, on voltage applied in the calibration circuit shown in Fig 5.

Table 1: The relation between the injected current, dose expressed in different units, and the input voltage on the calibration circuit.

Injected current	Dose per single PIN-diode	Input voltage, V
2.85 pA	1 rad/hour	—
285 pA	100 rad/hour = 1.667 rad/min = 27.8 mrad/s	0.323
1 nA	351 rad/hour = 5.85 rad/min = 97.5 mrad/s	1.131
171 pA	1 rad/min	0.194

5.3 Parameters of the Second Stage Filtered Amplifiers

The gain coefficients of the second stage Filtered Amplifiers have been measured at an input level $1 \pm 0.002\ V$. The results are listed in Table 3. The gains are equal to 10 with precision $\sim 3\%$. The observed dynamic range for their output is about $\pm 14\ V$.

5.4 Calibration of the gain

The response of the amplifiers and the ADCs is sequentially measured for the test input current 0 pA and ±285 pA, corresponding to a dose rate of 100 rad/hour/PIN diode.

Table 2: Measured filter parameters. R_s – resistance between signal pins of input and output connectors; R_g – resistance between grounds of input and output connectors; C_{out} – capacitance, measured at output connector; C_i – internal capacitance, measured directly in circuit.

Upper box, West				
N	R_s, k	R_g, k	$C_{out}, \mu F$	$C_i, \mu F$
1	104.3	106.2	1.11	1.12
2	104.2	105.4	1.06	1.14
3	105.3	107.2	1.12	1.09
4	108.0	105.4	1.16	1.11
5	104.1	103.1	1.09	1.06
6	106.6	104.7	1.08	1.10
7	104.5	105.1	1.08	1.11
8	106.9	103.1	1.05	1.09
9	106.7	106.2	1.08	1.10
10	104.8	106.6	1.13	1.13
11	106.4	105.8	1.06	1.13
12	105.4	108.0	1.02	1.13
Lower box, East				
1	107.4	107.0	1.10	1.13
2	106.4	106.7	1.07	1.12
3	105.3	104.9	1.10	1.11
4	104.4	107.3	1.12	1.12
5	106.4	104.8	1.10	1.16
6	106.0	103.6	1.12	1.15
7	106.7	105.1	1.14	1.12
8	104.4	105.4	1.11	1.11
9	107.2	106.3	1.11	1.06
10	104.8	102.7	1.12	1.11
11	104.9	103.2	1.08	1.08
12	103.4	102.6	1.12	1.12

To take in to account the shift of the base level due to the influence of the calibration circuit the responses for both signs of current was used. The typical responses of the west ring channels, for example, during the calibration are shown in Figure 8. The measured responses of the amplifiers and the ADCs are listed in Table 4. The calculated calibration coefficients are shown in Table 5 and in Figure 9. The pedestal is defined as the signal level when there is no beam in or no injection to CESR. Comparison of the calibration coefficients from Table 5 with previous calibration, taken four days earlier and shown in Table 6, shows that the pedestal and signal response fluctuations are random and do not exceed 4 ADC counts. This value is considered the stability of calibration coefficients.

As discussed above the calibration circuit shifts the amplifier base level about -2 mV which corresponds to a pedestal shift of -10 ADC channels. This correction is used in the calculation of the conversion coefficients.

Table 3: Measured voltage gain for the Gain 10 Filtered Amplifiers. Input voltage at measurement was set equal to 1 V with precision of 0.2%.

N	Upper box, West 1–8	Middle box, West 9–12, East 1–4	Lower box, East 5–12
1	9.95	9.95	9.81
2	10.04	10.06	9.78
3	9.99	10.17	9.80
4	9.94	10.58	10.85
5	9.99	10.26	9.79
6	10.00	9.90	9.62
7	10.00	9.89	9.77
8	9.94	9.89	9.80

Table 4: Response of amplifiers, high and low gain ADC channels on an injected current of $\mp 285 \pm 1$ pA, corresponding to 100 rad/hour

Channel	Amplifier response		High gain channels		Low gain channels	
No.	mV	mV	ADC count	ADC count	ADC count	ADC count
1W	251	-258	1524	-1503	150	-153
2W	257	-264	1587	-1523	153	-158
3W	261	-265	1582	-1563	156	-158
4W	258	-264	1563	-1536	154	-158
5W	257	-264	1551	-1565	153	-158
6W	258	-264	1569	-1548	153	-158
7W	249	-255	1516	-1500	148	-153
8W	258	-263	1549	-1554	154	-158
9W	253	-258	1542	-1487	150	-155
10W	253	-262	1551	-1541	151	-156
11W	248	-256	1524	-1539	147	-153
12W	248	-253	1608	-1553	148	-150
1E	247	-253	1528	-1542	147	-150
2E	269	-273	1599	-1607	160	-162
3E	251	-255	1486	-1511	148	-152
4E	240	-249	1446	-1440	142	-147
5E	258	-261	1516	-1526	153	-155
6E	262	-265	1534	-1557	156	-158
7E	263	-265	1542	-1547	156	-158
8E	252	-257	1641	-1656	150	-153
9E	247	-254	1455	-1485	147	-152
10E	260	-264	1429	-1431	154	-158
11E	259	-266	1518	-1556	154	-158
12E	271	-271	1581	-1595	160	-161

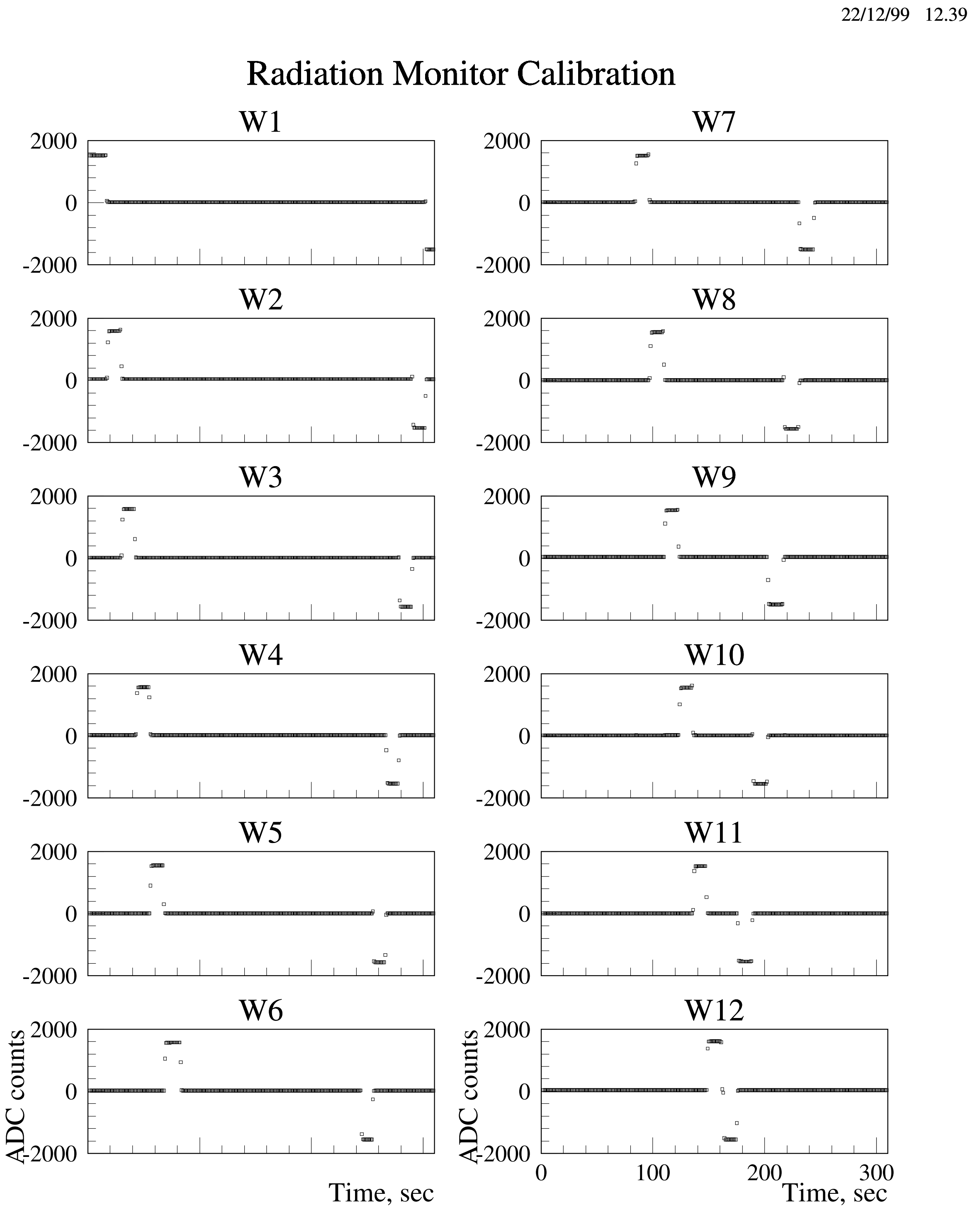

Figure 8: High gain channel response during the calibration procedure.

Within the precision of the digitization, all circuits demonstrate the linear response to injected test current.

5.5 Charge calibration of amplifier

Charge calibration has been done in order to verify that the calibration circuit in Figure 5 does not influence the amplifier gain. This approach also allows us to measure the timing

Table 5: Calibration coefficients for PIN-Diode Radiation Monitor electronics channels.

	Amplifier	High gain channels			Low gain channels	
Channel No.	Gain, $\frac{V}{nA}$	Pedestal, ADC count	Gain, $\frac{ADC\ count}{mV}$	Dose coef., $\frac{mrad}{min \cdot ADC\ count}$	Gain, $\frac{ADC\ count}{mV}$	Dose coef., $\frac{mrad}{min \cdot ADC\ count}$
1W	0.893	19	5.95	1.101	0.595	11.0
2W	0.914	43	5.97	1.072	0.597	10.7
3W	0.923	16	5.98	1.060	0.597	10.6
4W	0.916	22	5.94	1.076	0.598	10.7
5W	0.914	4	5.98	1.070	0.597	10.7
6W	0.916	19	5.97	1.069	0.596	10.7
7W	0.884	16	5.98	1.105	0.597	11.1
8W	0.914	6	5.96	1.074	0.599	10.7
9W	0.896	37	5.93	1.100	0.597	10.9
10W	0.904	18	6.00	1.078	0.596	10.9
11W	0.884	6	6.08	1.088	0.595	11.1
12W	0.879	36	6.31	1.055	0.595	11.2
1E	0.877	3	6.14	1.086	0.594	11.2
2E	0.951	4	5.92	1.040	0.594	10.4
3E	0.888	-3	5.92	1.112	0.593	11.1
4E	0.858	15	5.90	1.155	0.591	11.5
5E	0.911	1	5.86	1.096	0.593	10.8
6E	0.925	-3	5.87	1.078	0.596	10.6
7E	0.926	3	5.85	1.079	0.595	10.6
8E	0.893	1	6.48	1.011	0.595	11.0
9E	0.879	-3	5.87	1.134	0.597	11.1
10E	0.919	4	5.46	1.166	0.595	10.7
11E	0.921	-9	5.86	1.084	0.594	10.7
12E	0.951	-5	5.86	1.050	0.592	10.4

parameters of the amplifiers and to estimate their voltage-to-charge and voltage-to-current gain factors.

Rectangular pulses from Datapulse 100A Pulse Generator with amplitude $U_{\rm in}$ = +10 V, duration $\sim$ 100 ms, and repetition time 2.5 s were used as input the the calibration circuit shown in Figure 6. This circuit inject the charge $\Delta q = CU_{in} = \pm 100$ pC into the amplifier at each front of rectangular pulse. Typical oscilloscope diagram observed at exit of the amplifier with 50 ohm termination is shown in Figure 10. There is little response variation from channel to channel. Based on this diagram, main parameters of the amplifier can be estimated. Each front gives the jump of the output level $\Delta U_{\rm out} =^{-300\ {\rm mV}}_{+345\ {\rm mV}}$. Relaxation time is estimated to be $\tau = 250$ ms. Hence, the charge to voltage and current to voltage gain factors could be evaluated:

$$G(q \to V) = \Delta U_{out}/\Delta q = 3.45\ mV/pC,$$

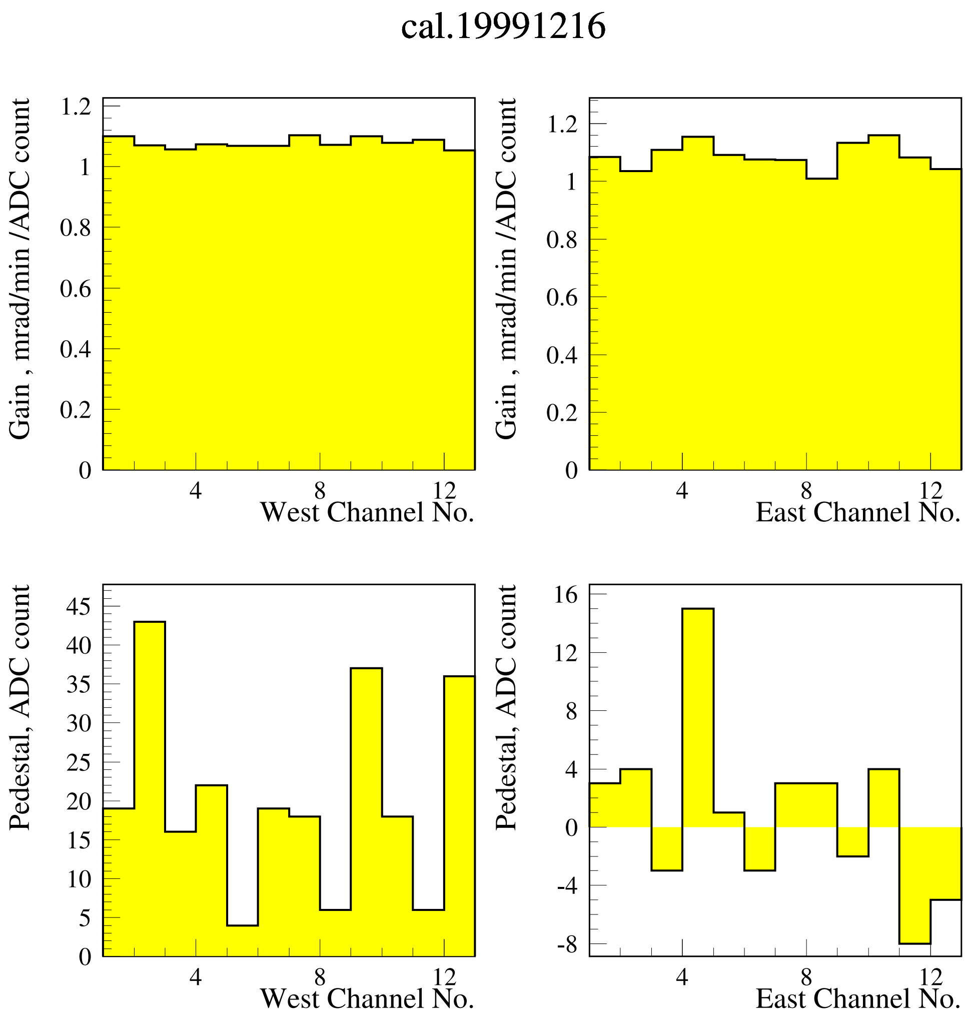

Figure 9: Gain coefficients and pedestals for the radiation monitor system.

$$G(I \to V) = \Delta U_{out} \cdot \tau / \Delta q = 0.86 \ V/nA.$$

Within precision of measurement the last gain factor coincides well with data obtained from normal current calibration shown in Table 5.

6 Temperature dependence of pedestal level

A dedicated study has been done to estimate the dependence of pedestal level on temperature of the beam pipe close to the PIN-diodes location. This was a problem in the CLEO II.V era when the same radiation monitor system was in place. The temperature of the beam pipe was changed steadily by varying the set point on the CLEO beampipe cooling system from 20 to 26^{o}C. The mean temperature for different groups of beam-pipe

Table 6: Response and calibration coefficients for PIN-Diode Radiation Monitor high gain electronics channels, measured on December 16, 1999, at injected current $-285 \pm 1\ pA$, corresponding to 100 rad/hour.

Channel N	Pedestal, ADC count	Response, ADC count	k, $\frac{mrad}{min \cdot ADC count}$
1W	19	1525	1.099
2W	43	1590	1.070
3W	16	1584	1.056
4W	22	1566	1.073
5W	4	1554	1.068
6W	19	1570	1.068
7W	18	1519	1.103
8W	6	1551	1.072
9W	37	1543	1.099
10W	18	1554	1.078
11W	6	1527	1.089
12W	36	1609	1.053
1E	3	1530	1.084
2E	4	1605	1.035
3E	-3	1491	1.108
4E	15	1450	1.153
5E	1	1519	1.091
6E	-3	1537	1.075
7E	3	1545	1.074
8E	3	1645	1.009
9E	-2	1459	1.133
10E	4	1432	1.159
11E	-8	1521	1.083
12E	-5	1584	1.042

thermocouple sensors during this period is shown in Figure 11. Corresponding variation of pedestal level measured for few high gain channels of radiation monitor is shown in Figure 12. Some channels show very slow dependence ~ 1 ADC count/5^{o}C, that is small compared to the stability of the gains. Variation of the beam-pipe temperature during CESR runs, for example see Figure 13, does not exceed 2^oC. The temperature dependence is negligible and no correction is made for it. Apparently the new PIN-diodes have a much reduced dark current versus temperature, the source of the temperature dependence in the old system.

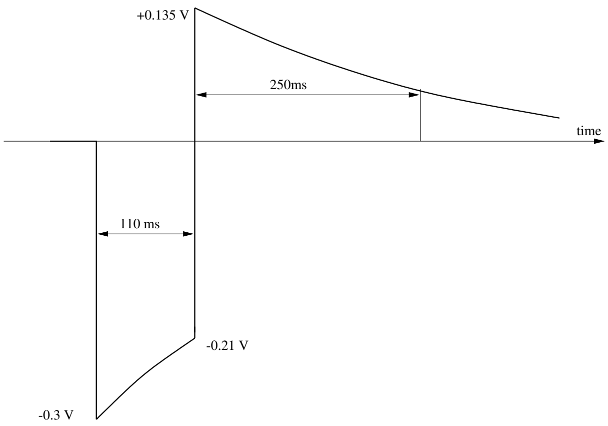

Figure 10: Typical response of the amplifier for short charge signals, obtained with calibration circuit shown in Fig 6.

7 Correlations of monitor response with a beam current

It is important to show that the radiation monitor system really sees the radiation from beam current in CESR rather than being dominated by background fluctuations.

The response one of the radiation monitor channels is shown in Figure 14 as a function of time. The radiation signal accurately tracks the beam current. The bottom two plots in Figure 14 show the correlations between beam current and response of the first channel for west and east rings. The correlation is obvious and we conclude that the PIN-diode Radiation Monitor can be used for optimization of CESR beam induced background in CLEO.

8 Integrated dose

Based on calibration coefficients listed in Table 5 we calculated the integrated radiation dose for the CLEO III engineering run November 6, 1999 through February 7, 2000. Shown in Figure 15 is the integrated dose averaged over all PIN-diodes versus time. The histograms show the total integrated dose on each PIN-diode. The enhancement in the median plane of the ring is evidence for a substantial amount of synchrotron radiation being scattered off the masks tips at 25 cm from the interaction point.

9 Conclusion

The radiation monitor system at the end of the CLEO III engineering run is in a good working condition. The calibration of the electronics channels has been done and the procedures are easy to repeat to monitor the system. The integrated dose can be calculated for any desirable period of time. The only change in the system is to install a new set of PIN-diodes that were long ago installed on the CLEO III beryllium beam pipe, around which the Si3 was built. The environment of the diodes will change. Instead of being

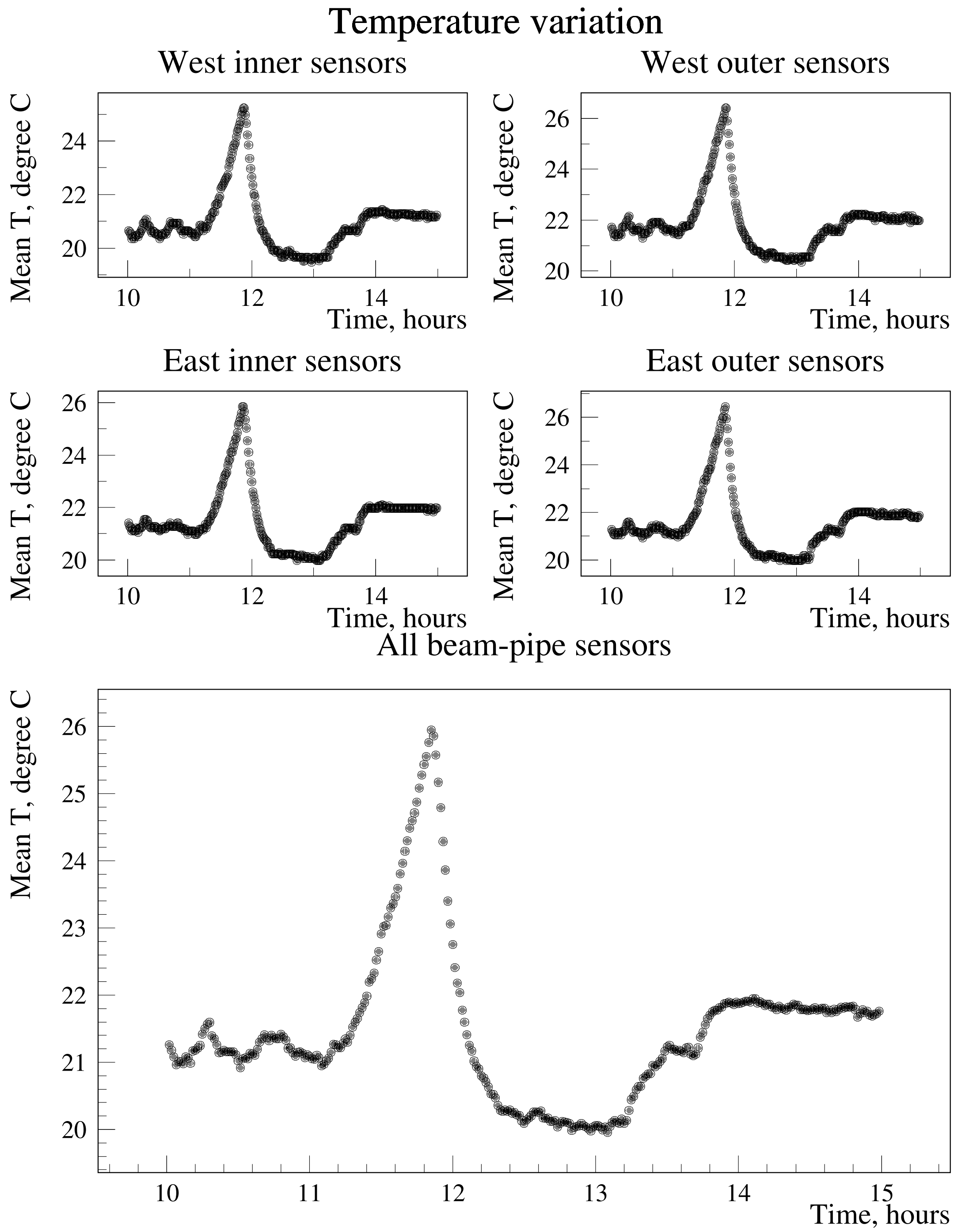

Figure 11: Variation of the beam-pipe temperature. Each point corresponds to 1 min.

behind the 1/8" of aluminum of Pipe 0, they will be behind a thin beryllium pipe and a thin layer of gold. Every other diode will be shielded from synchrotron radiation by a 0.1 mm layer of platinum to allow us to observe the synchrotron radiation signal directly by subtraction.

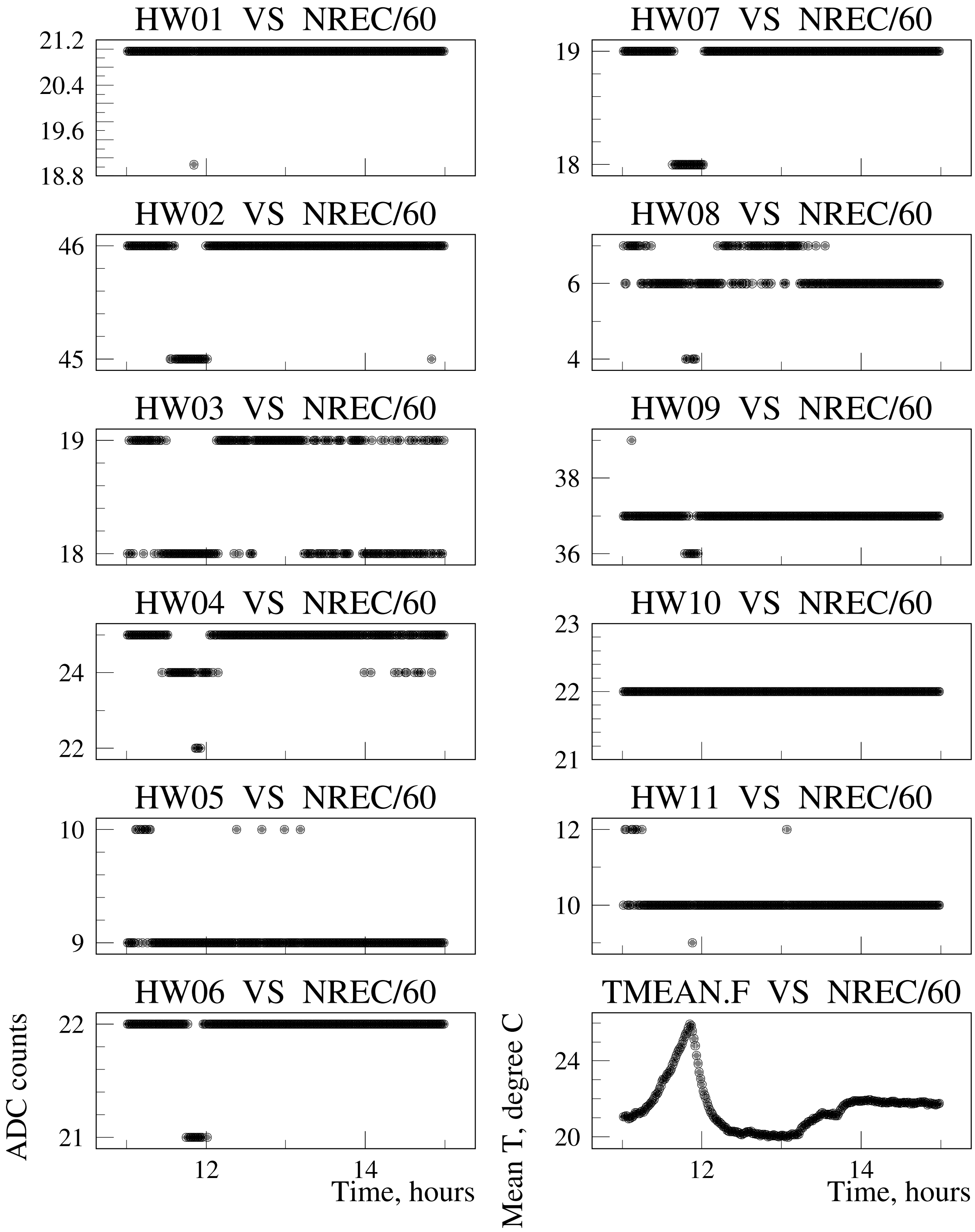

Figure 12: Variation of pedestals as the beampipe temperature is varied. Occasionly the pedestals fluctuate by 2 ADC count due to a 1.5 gain factor applied to the raw signal to the read ADC response.

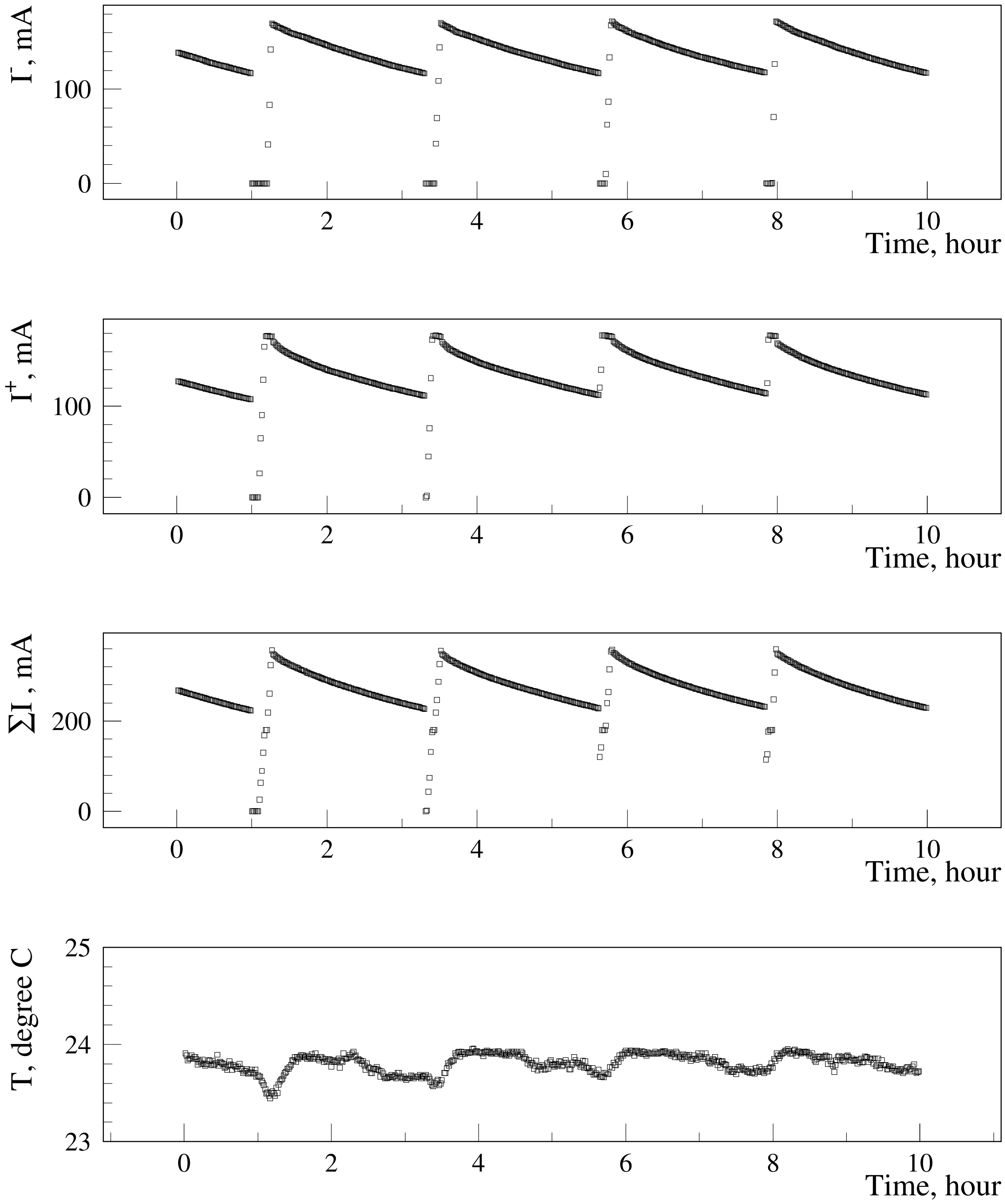

Figure 13: Beam currents and mean beam-pipe temperature during the owl shift of 12/20/99.

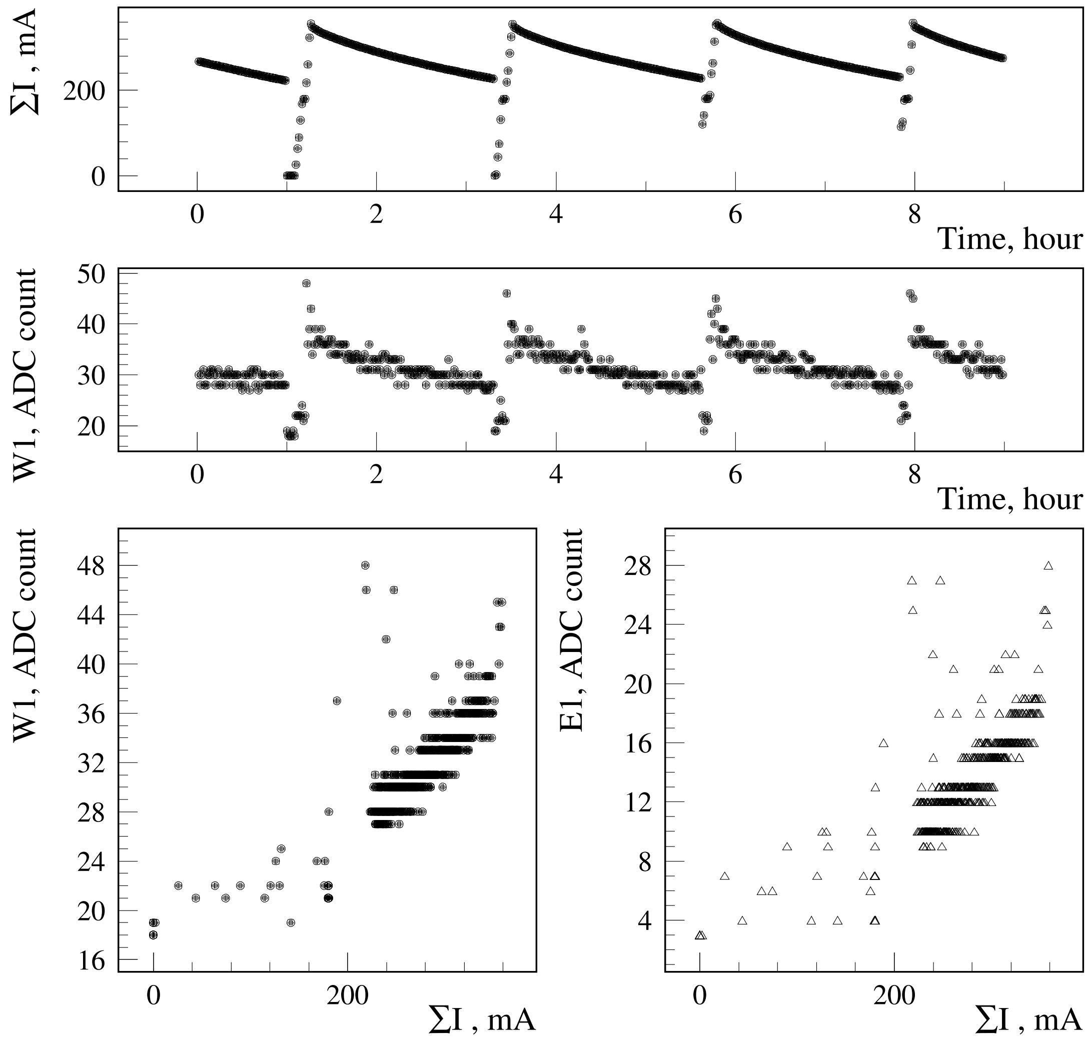

Figure 14: Correlations of radiation monitor response with beam current. Each point corresponds to 1 min. Data from owl shift 12/20/99.

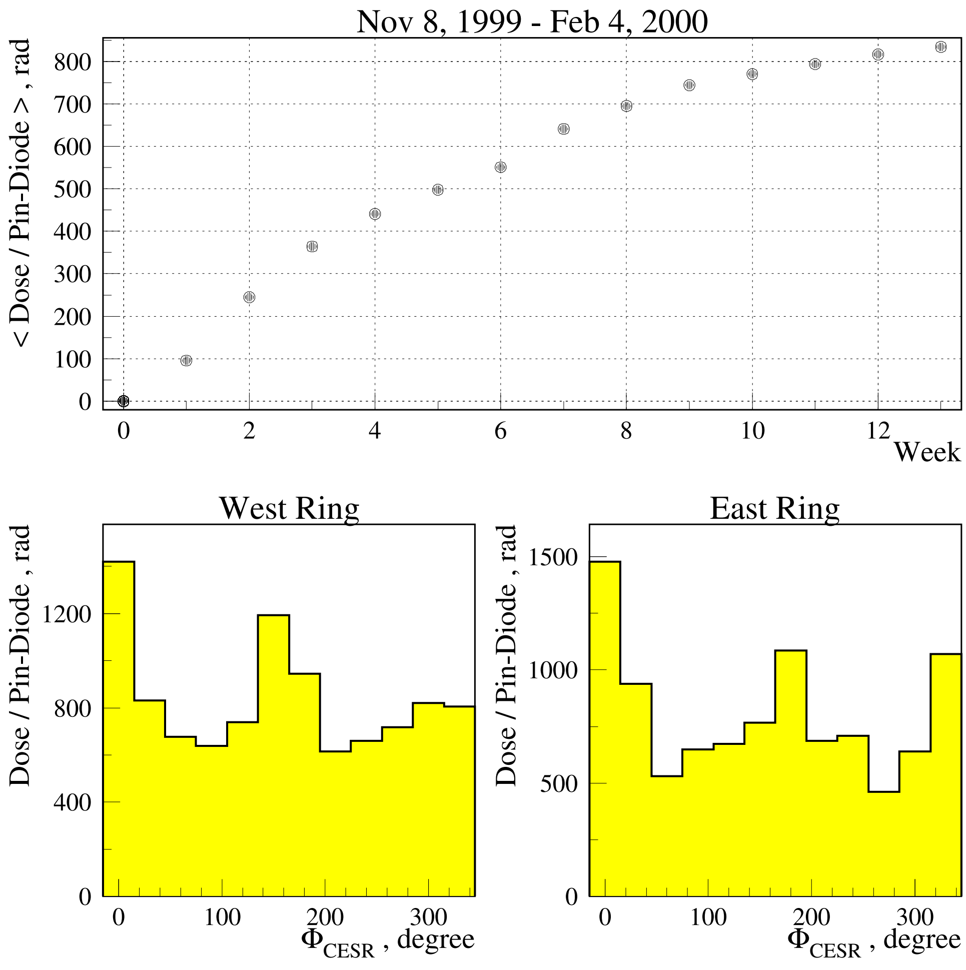

Figure 15: The PIN-diode radiation monitor dose integrated during the CLEO III engineering run. The upper plot shows the average dose versus time and the lower histograms shows the total integrated does on each diode.